Journal of Structural Geology 74 (2015) 172–184

Contents lists available at ScienceDirect

Journal of Structural Geology

journal homepage: www.elsevier.com/locate/jsg

Contractional deformation of porous sandstone: Insights from the Aztec Sandstone, SE Nevada, USA

Haakon Fossen [a, b, *], Luisa F. Zuluaga [a, c], Gregory Ballas [d], Roger Soliva [d], Atle Rotevatn [a]

[a] Department of Earth Science, University of Bergen, Allégaten 41, N-5007 Bergen, Norway
[b] Museum of Natural History, University of Bergen, Allégaten 41, Postboks 7800, N-5020 Bergen, Norway
[c] Centre for Integrated Petroleum Research (Uni CIPR), Allégaten 41, 5007 Bergen, Norway
[d] Laboratoire Géosciences Montpellier, University Montpellier, Place Eugène Bataillon, 34000 Montpellier, France

ARTICLE INFO

Article history:
Received 6 October 2014
Received in revised form
19 February 2015
Accepted 26 February 2015
Available online 19 March 2015

Keywords:
Sevier thrusting
Porous sandstone deformation
Deformation bands
Contractional deformation

ABSTRACT

Contractional deformation of highly porous sandstones is poorly explored, as compared to extensional deformation of such sedimentary rocks. In this work we explore the highly porous Aztec Sandstone in the footwall to the Muddy Mountain thrust in SE Nevada, which contains several types of deformation bands in the Buffington tectonic window: 1) Distributed centimeter-thick shear-enhanced compaction bands (SECBs) and 2) rare pure compaction bands (PCBs) in the most porous parts of the sandstone, cut by 3) thin cataclastic shear-dominated bands (CSBs) with local slip surfaces. Geometric and kinematic analysis of the SECBs, the PCBs and most of the CSBs shows that they formed during ~E–W (~100) shortening, consistent with thrusting related to the Cretaceous to early Paleogene Sevier orogeny of the North American Cordilleran thrust system. Based on stress path modeling, we suggest that the compactional bands (PCBs and SECBs) formed during contraction at relatively shallow burial depths, before or at early stages of emplacement of the Muddy Mountains thrust sheet. The younger cataclastic shear bands (CSBs, category 3), also related to E–W Sevier thrusting, are thinner and show larger shear offsets and thus more intense cataclasis, consistent with the initiation of cataclastic shear bands in somewhat less porous materials. Observations made in this work support earlier suggestions that contraction lead to more distributed band populations than what is commonly found in the extensional regime, and that shear-enhanced compaction bands are widespread only where porosity (and permeability) is high.

1. Introduction

Most sandstones with porosity in excess of ca. 15% develop deformation bands during low-strain deformations in any tectonic regime (e.g., Davis, 1999; Fossen et al., 2007). The evolution of deformation bands during extensional tectonics has been extensively studied since the late 70s, particularly through investigations of deformed Jurassic sandstones of the Colorado Plateau (e.g., Aydin and Johnson, 1978; Antonellini and Aydin, 1994). The type of deformation band most commonly reported in the literature show shear-induced grain crushing and compaction in a 1–2 mm thick zone in the sandstone with up to a few cm of shear offset which, depending on the thickness of the band, typically amount to shear strains of 1–10 and 20–30% volume loss (e.g., Aydin and Johnson, 1978; Underhill and Woodcock, 1987; Antonellini and Aydin, 1994; Davis, 1999). Such bands are referred to as compactional shear bands (Fossen and Bale, 2007) or, combining their textural and kinematic characteristics, *cataclastic compactional shear bands* (CSBs). In addition, *non-cataclastic shear bands* with predominantly shear offsets are very common in the extensional regime, particularly where the burial depth at the time of deformation was low (<1 km) (Fisher and Knipe, 2001; Hesthammer and Fossen, 2001). Where developed in relatively pure sand(stone), such as the Aztec Sandstone studied in this work (see below), non-cataclastic bands do not develop significant porosity or volume changes, and hence do not alter the petrophysical properties of the rock. We will not consider this group of deformation bands in this work.

A characteristic feature of sandstone deformation in the extensional regime is the tendency for cataclastic deformation bands to cluster into decimeter-thick zones that may or may not evolve into faults (e.g., Antonellini and Aydin, 1994; Shipton and Cowie, 2003,

* Corresponding author. Department of Earth Science, University of Bergen, Allégaten 41, N-5007 Bergen, Norway.
E-mail address: haakon.fossen@geo.uib.no (H. Fossen).

http://dx.doi.org/10.1016/j.jsg.2015.02.014
0191-8141/

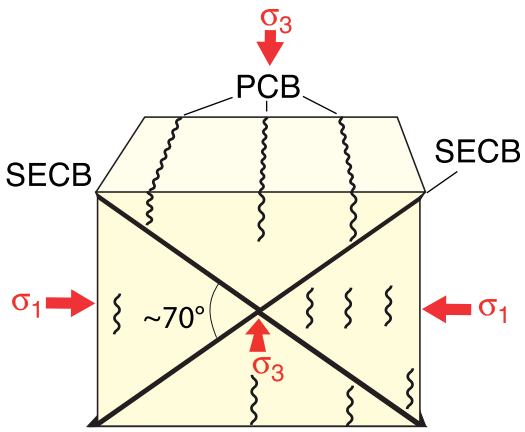

Fig. 1. Conceptual diagram demonstrating the spatial relationship between pure compaction bands (PCB), shear-enhanced compacion bands (SECB) and the principal stress directions.

Johansen and Fossen, 2008). Fault evolution happens through the formation of a slip surface that accumulate most of the offset, and which is contained within a zone of partly pre-existing deformation bands. Such cataclastic deformation band zones can represent tabular rock volumes where porosity is reduced by more than one order of magnitude and permeability by up to 3–5 orders of magnitude (Antonellini and Aydin, 1994; Fossen and Bale, 2007).

Much less work has been done on contractional deformation of highly porous sandstones. In addition to mm-thick cataclastic (compactional) shear bands (CSBs), *shear-enhanced compaction bands* (SECBs) and *pure compaction bands* (PCBs) are found in the contractional tectonic regime (Eichhubl et al., 2010; Fossen et al., 2011; Ballas et al., 2013). Such bands are reported from the Valley of Fire State Park, Nevada (Sternlof et al., 2005; Tembe et al., 2008), where they both were called compaction bands until Eichhubl et al. (2010) suggested that they are kinematically different, and therefore relate differently to principal axes of stress and strain. Specifically, PCBs form perpendicular to the shortening direction or the maximum compressional stress direction (σ_1), while SECBs form oblique to this direction, typically in the form of two conjugate sets bisected by σ_1 (Fig. 1). SECBs are notably thicker (cm-scale) than the mm-thick cataclastic bands (CSBs) widely reported from extensional settings, and show much smaller (typically less than 1 mm) shear offsets that are quantitatively comparable to the compaction-induced offsets (Eichhubl et al., 2010). It has also been suggested that shortening of porous sandstones generates more distributed arrays of bands than what is typically seen in the extensional regime (Solum et al., 2010). This was explored in detail by Ballas et al. (2012, 2013), who studied poorly consolidated porous sandstones in Provence, France. In this area, extensional deformation generated deformation band clusters that developed into normal faults, whereas the preceding contraction created much more evenly distributed SECBs and CSBs without any obvious relationship to faults (Saillet and Wibberley, 2010; Soliva et al., 2013).

In general, it should be emphasized that particular interest is devoted to deformation bands in hydro, CO_2 or petroleum reservoirs because of their associated reduction in porosity and permeability, which again potential effect on reservoir performance (e.g., Sternlof et al., 2006). Although bands and clusters have a theoretical sealing capacity of several tens of meters (Torabi et al., 2013), they are rarely completely continuous in three dimensions for a sufficiently long distance to act as trap-forming elements, and hence only have baffling effects on fluid flow in most cases (e.g., Sternlof et al., 2006; Fossen and Bale, 2007; Rotevatn and Fossen, 2011). Their effect on the bulk petrophysical properties of the sandstones depends on their permeability reducing properties, thickness, density (frequency) and thickness, while their orientation, geometry and distribution control their ability to divert fluid flow during reservoir production and injection.

In the present contribution we will examine an area where porous Aztec Sandstone has been shortened and overridden by a several kilometer thick Sevier-age thrust sheet. The aim is to explore how porous sandstone responds to contractional deformation that leads to the emplacement of a thrust nappe on top of the sandstone, and to add to our understanding of sandstone deformation in the contractional regime in general. Finally, the implications for the findings are discuss in terms of reservoir performance. For a discussion of the deformation along the thrust fault itself, see Brock and Engelder (1977).

2. Geologic setting

The focus of this study is the Jurassic Aztec Sandstone, which is part of an extensive eolian sandstone unit called the Navajo and Nugget sandstones on the Colorado Plateau to the east and north. The Aztec Sandstone was involved in Sevier thrusting in Nevada

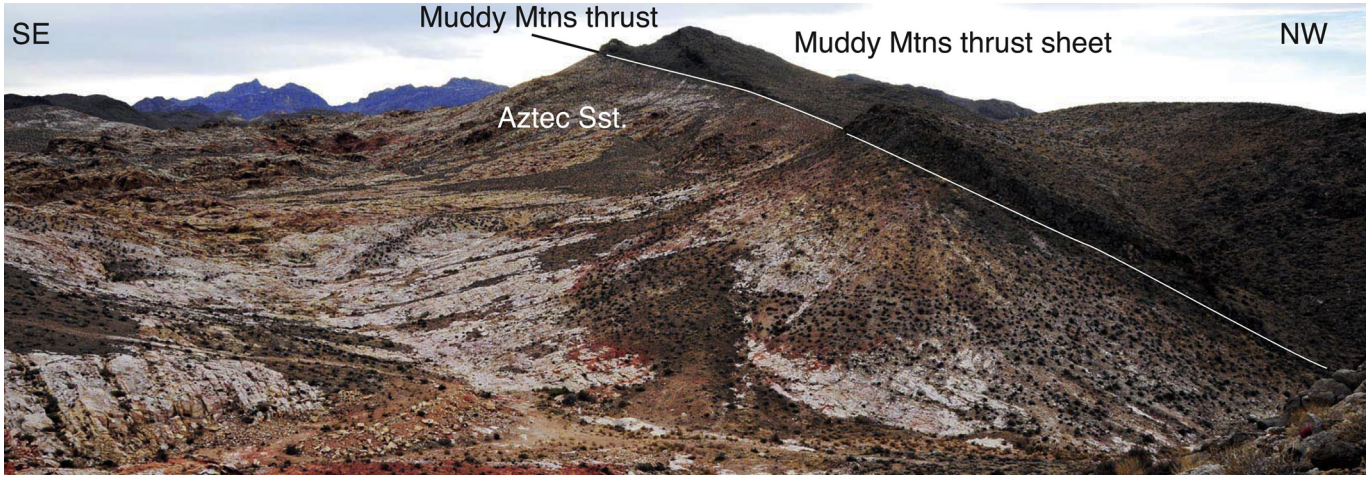

Fig. 2. The Muddy Mountains thrust separating Aztec Sandstone (footwall) from Paleozoic carbonate-rich rocks in the hanging wall (right). The contact has been rotated during Basin and Range normal faulting.

and western Utah, and is exposed in the tectonic Buffington window underneath Paleozoic rocks of the Muddy Mountains thrust sheet (Fig. 2), and in the Valley of Fire State Park to the north-east (Fig. 3).

The primary study area is the Buffington tectonic window, which exposes around 28 km^2 of porous Aztec Sandstone underneath the Muddy Mountains thrust. The thrust contact against mostly dolomites and limestones of the Bonanza King Formation in the lower part of the overlying thrust sheet is described by Brock and Engelder (1977). In short, the Aztec sandstone has developed a meter-thick zone of strong cataclastic deformation and grain pressure solution that reduce porosity to almost zero along the contact. However, some meters or tens of meters downward into the sandstone it can reach porosities up to 20–25% (thin section estimates) and permeabilities of several darcy (as measured with a portable air permeameter) (Zuluaga, 2015).

Following the Sevier contraction, the region was affected by Basin and Range extensional tectonics, as manifested by a large number of extensional faults offsetting the Muddy Mountains thrust contact and tilting the thrust and the Aztec Sandstone (Fig. 3). Transcurrent fault systems, notably the Las Vegas Valley shear zone, accompanied the Basin and Range extension, but had only limited influence on the Buffington Window area. The general current dip of the Aztec Sandstone in the window is around 20° to the southeast, implying that pre-Cenozoic structures should be rotated correspondingly.

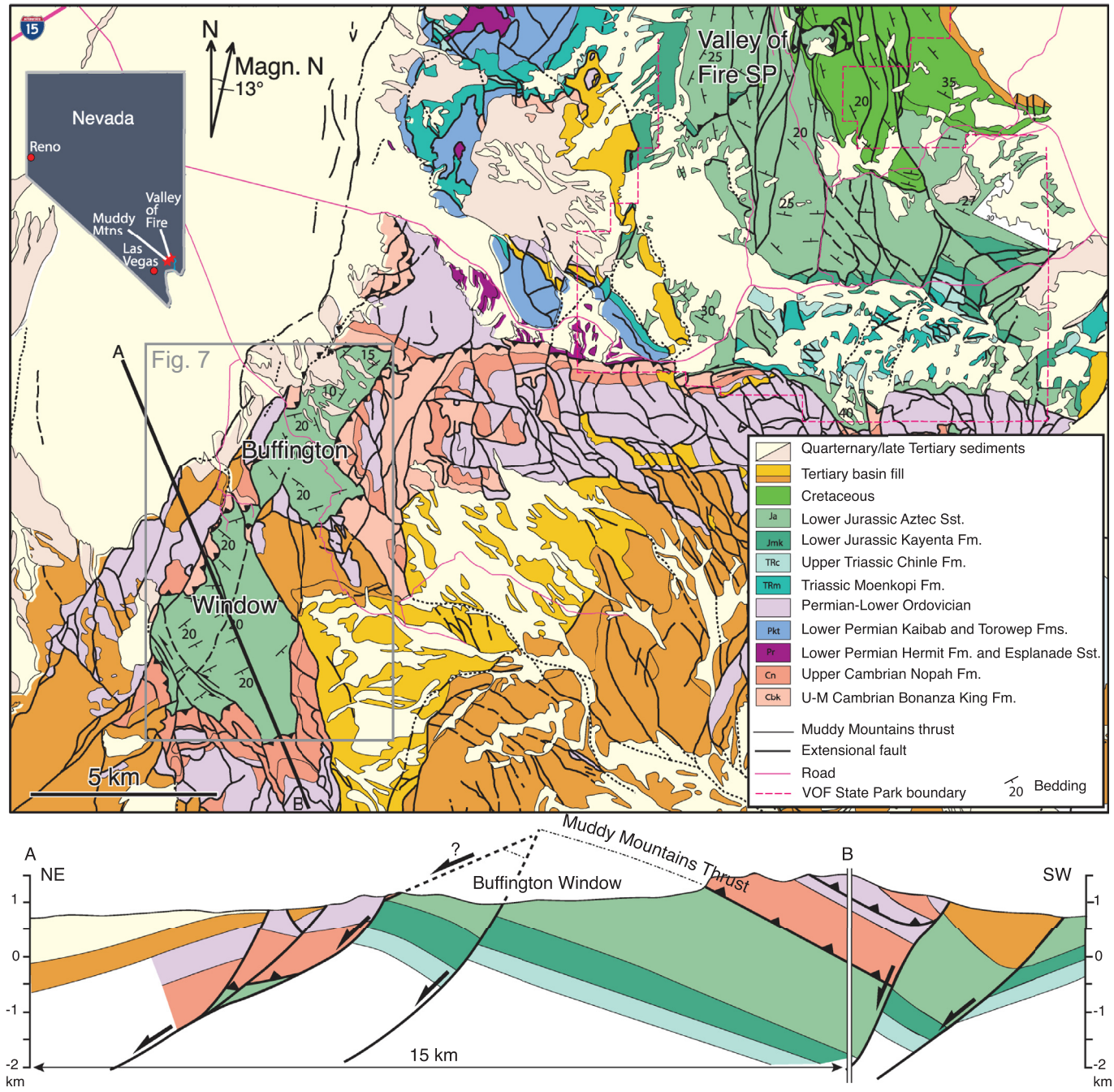

Fig. 3. Geologic map and cross section of the Buffington Window and Valley of Fire area, SE Nevada. Based on Bohannon (1983).

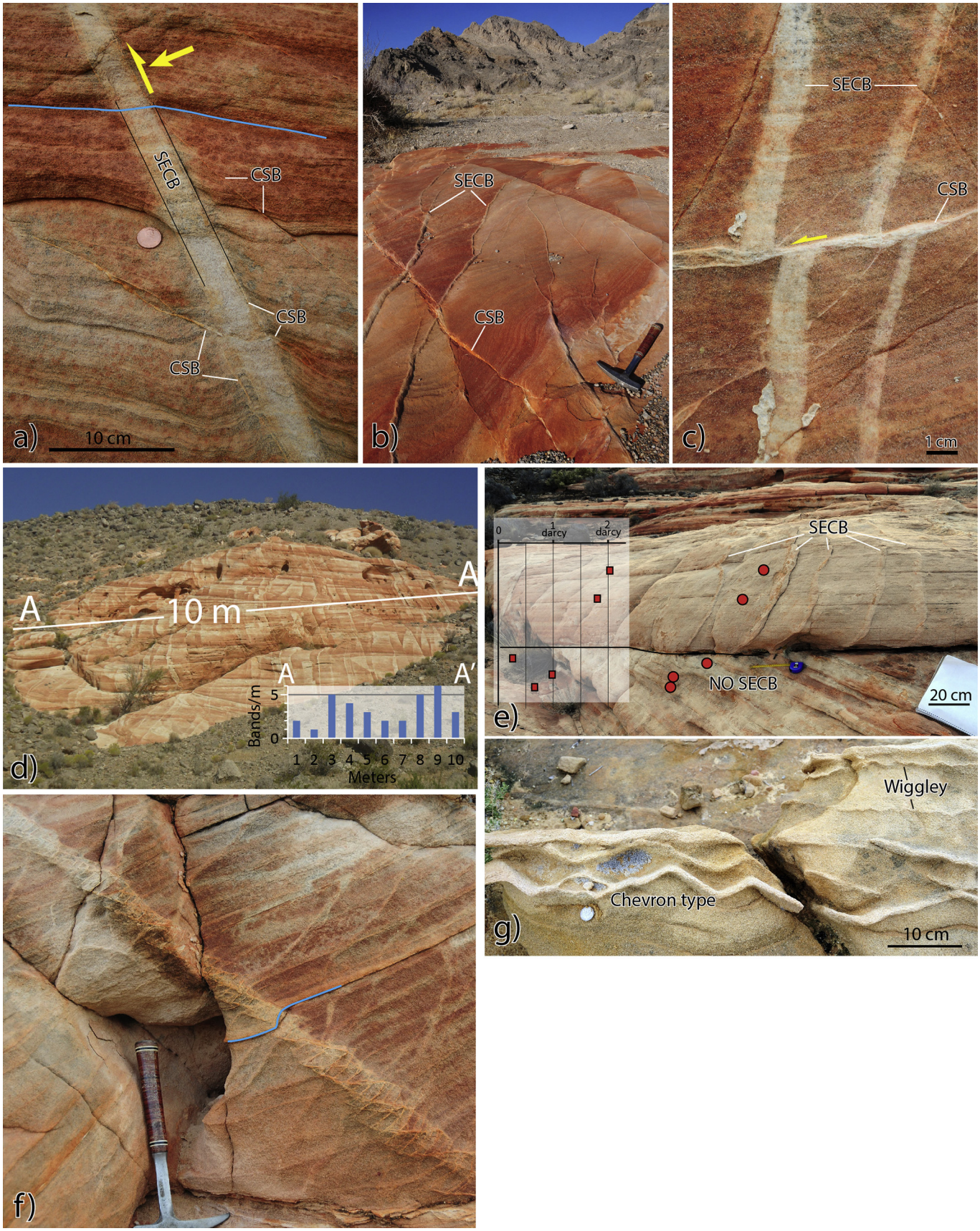

Fig. 4. a) Shear-enhanced compaction bands (SECB), showing only slight reverse offset of bedding. Coin is 1.9 cm in diameter. b) SECB on subhorizontal surface, showing evidence of growth by linkage. c) Thin zone of cataclastic shear bands (CSBs) offsetting two SEDBs. d) Population of SECBs with an average spacing around 3 m^{-1}. e) A parallel set of planar SECB limited to the highly porous/permeable lower part of a dune unit. f) Ladder structure with reverse offset, constructed by CSBs. g) Wiggley and chevron types of pure compaction bands, Valley Of Fire.

3. Structural observations

The Aztec Sandstone in the Buffington Window exhibits three distinctly different types of deformation bands; pure compaction bands (PCBs), shear-enhanced compaction bands (SECBs) and cataclastic compactional shear bands (CSBs). These band types are distinguished on the basis of geometry, kinematics, thickness and deformation mechanisms.

3.1. Pure compaction bands

Structures recognized as PCBs in the Buffington Window – Valley of Fire area are 0.5–2 cm thick bands characterized by non-planar geometries, commonly showing wiggly or chevron-style geometries (Fig. 4g). No offset is seen across PCBs, and they are only observed sporadically, and only in the most porous and permeable parts of the Aztec sandstone. This is consistent with observations from the Navajo Sandstone in Utah where they only form in sandstones with porosity around 30% or more and permeability in excess of 10 darcy (Fossen et al., 2011). On the microscale, PCBs involve only a limited amount of cataclasis, similar to CSBs described from Valley of Fire (Eichhubl et al., 2010), but somewhat less than those described from southern Utah (Mollema and Antonellini, 1996; Fossen et al., 2011). They are more common in highly porous and permeable layers in Valley of Fire, where they occur in parts of the sandstone where porosity reaches 20–25% (estimated from thin sections), and 2–15 darcy permeability (Fig. 5) based on measurements using a portable probe permeameter (TinyPerm-II); see Rotevatn et al., 2008 for details on the method and Fossen et al., 2011 for calibration against plug measurements). The PCBs form high angles to bedding and dip steeply to the WNW throughout the Buffington Window area (Figs. 6 and 7), with very similar orientations to those found in the Valley of Fire (compare Fig. 6a and d). This orientation is consistent with an ESE-WSW shortening direction (see below).

3.2. Shear-enhanced compaction bands

The SECBs are cm-thick structures that typically show a very planar geometry (Fig. 4a, c, d and e), although curvature related to linkage structures can sometimes be seen in horizontal sections (Fig. 4b). They record very small (mm-scale or less) offsets that may be difficult to see, depending on their orientation with respect to the local lamination. Where offset is seen, it appears reverse in cross-section (Fig. 4a). Microstructurally the SECBs contain fractured grains (Figs. 8 and 9a, b), interpreted as evidence of cataclasis. The density of fractures in the grains is moderate, varying from survivor grains that show no fractures (Figs. 8b and 9a) to grains that are broken up into multiple pieces (Fig. 9b). We also see that some quartz grains “intrude” into neighboring quartz grains (Fig. 9a) in a way that is characteristic of pressure solution at grain contacts. In contrast, evidence for quartz cement is scarce. Both the cataclasis and pressure solution involve compaction and thus reduce porosity and permeability within the SECBs. Probe permeameter measurements were performed on host rock (parallel to bedding) and across deformation bands, and the results show that the reduction in permeability imposed by the deformation bands ranges from none to 2.8 orders of magnitude (Fig. 10). The largest reductions were recorded in bands where dissolution and grain fracture are prominent. These observations are similar to those of SECBs measured in Buckskin Gulch, Utah by Fossen et al. (2011).

The SECBs define two sets, where the majority of the SECBs dip steeply to the ESE (020/63E on average). This dominating set can be observed along several ten-meters long outcrops as quite well organized network showing an average band thickness of about 11.6 ± 7.6 mm (N = 41), an average band spacing of about 0.315 ± 0.2268 m (N = 40) and a corresponding average band density of 3.3 bands/m (Fig. 4d). The other set is less well defined, and dips in the opposite direction (197/27W on average). The bands of this set are locally parallel to dune foreset lamina similar to SECBs described by Mollema and Antonellini (1996) in southern Utah and by Aydin and Ahamadov (2009) in the Valley of Fire area. Some variations are seen between different localities (Fig. 7), and at some outcrops the bands show a variation in strike that in part can be related to band growth by segment linkage (SECB in Fig. 4b) (e.g., Fossen and Hesthammer, 1997). These variations are reflected by the scatter portrayed in the stereoplots (Figs. 6b and 7). In general, individual dune sets show only one of the two conjugate sets, as described by Deng and Aydin (2012) at Valley of Fire, and only a few dune units show both sets.

On a large scale, the occurrence of SECBs is restricted to the central and eastern part of the basin. Their absence closer to the western contact may be related to stronger cementation in this part of the window, since cementation and related porosity loss can restrict deformation band formation. This would imply that at least some of the cement was formed at the time of band formation, which we are not able to confirm at this point. There is also a tendency for the second set of bands to be better developed in the southern part of the window than in the northern part (Fig. 7).

On outcrop scale, the distribution of SECBs is influenced by the original porosity and grain size of the sandstone. Fossen et al. (2012) showed that both SECBs and PCBs are preferentially developed in the best sorted, most coarse-grained and most permeable layers of the Navajo Sandstone in southern Utah, which for eolian systems is the lower part of the sand dune deposits (excluding the base of the dune). A similar relationship is seen in the Aztec sandstone in the present study area, as illustrated the inset graph in Fig. 4e showing permeability measurements. Fig. 5 shows that SECBs only occur in sandstones with permeability greater than ~1 darcy. This is very similar to observations made in the Navajo

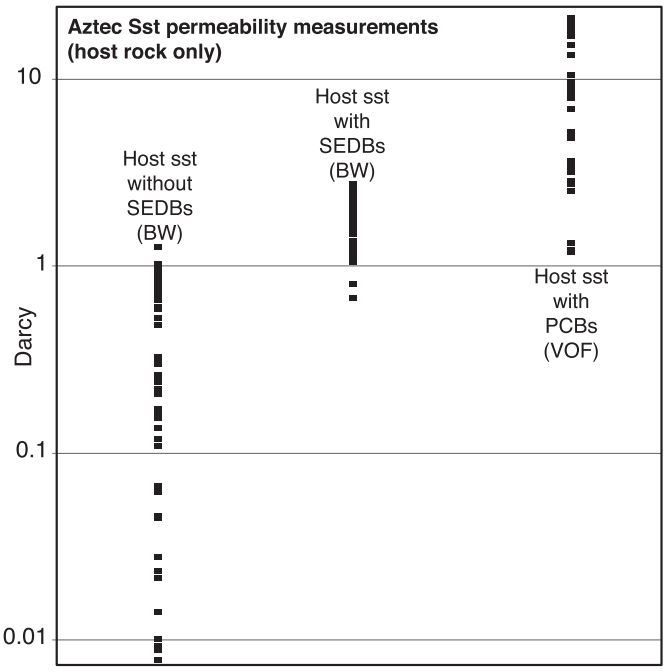

Fig. 5. Permeability measurements of Aztec sandstone void of shear-enhanced deformation bands (SEDBs) (left), hosting SEDBs (middle) and hosting PCBs (PCB s from Valley of Fire, all other measurements from the Buffington Window).

Sandstone in southern Utah by Fossen et al. (2011). However, post-deformation burial has reduced porosity and permeability somewhat since the time of deformation, hence these are minimum values for the rock properties required for SEDBs to form. Nevertheless, it shows clearly that the distribution of SECBs is strongly influenced by lithology and sedimentary facies, which is useful knowledge when trying to predict and model such structures in a subsurface reservoir.

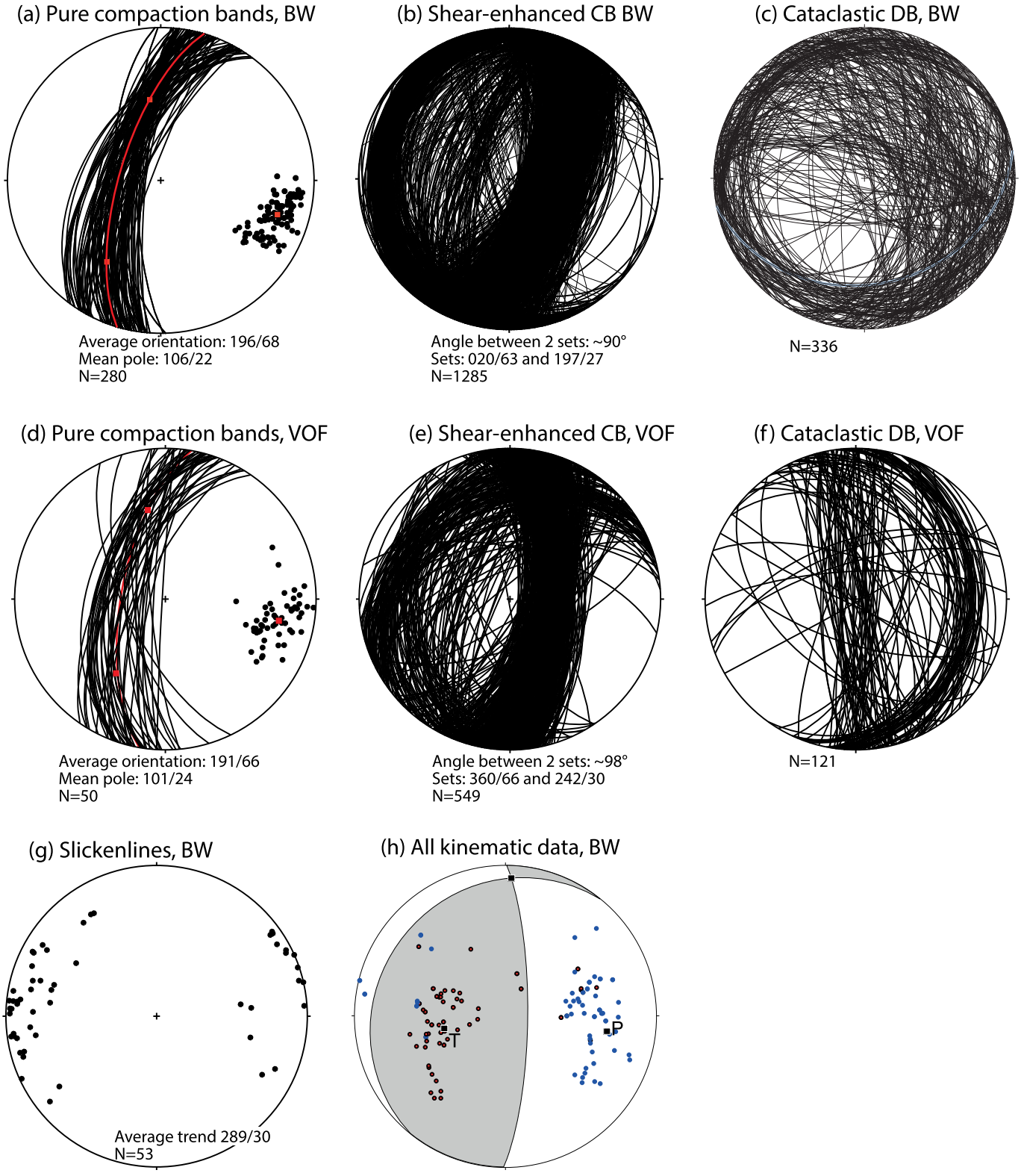

Fig. 6. Stereoplots of pure compaction bands (PCB), shear-enhanced deformation bands (SEDB), Cataclastic deformation bands (CB), slickenlines and kinematic data from slipped cataclastic deformation bands. From the Buffington Window (a–c and g–h) and Valley of Fire (d–f).

3.3. Cataclastic compactional shear bands

Cataclastic compactional shear bands (CSBs), i.e. cataclastic bands with predominantly shear displacement, are around 1 mm thick and show cm-scale offsets that consistently transect and thus postdate the PCBs and SECBs (Fig. 4c). The bands show a fairly wide range in orientation with a steep prominent set and another set dipping gently to the E (Fig. 6f). Offsets are contractional with respect to bedding, i.e. reverse when removing the rotation associated with the Basin and Range block faulting (see Fig. 3, cross-section). Some of these CSBs are deflected close to SECBs, bending into parallelism with the SECB and following their margins (Fig. 4a), while others cut straight through, locally in thin clusters as the one seen in Fig. 4c. They are observed sporadically in the window where porous sandstones are observed, also in foresets of dunes where SECBs and PCBs are not observed, without any well-

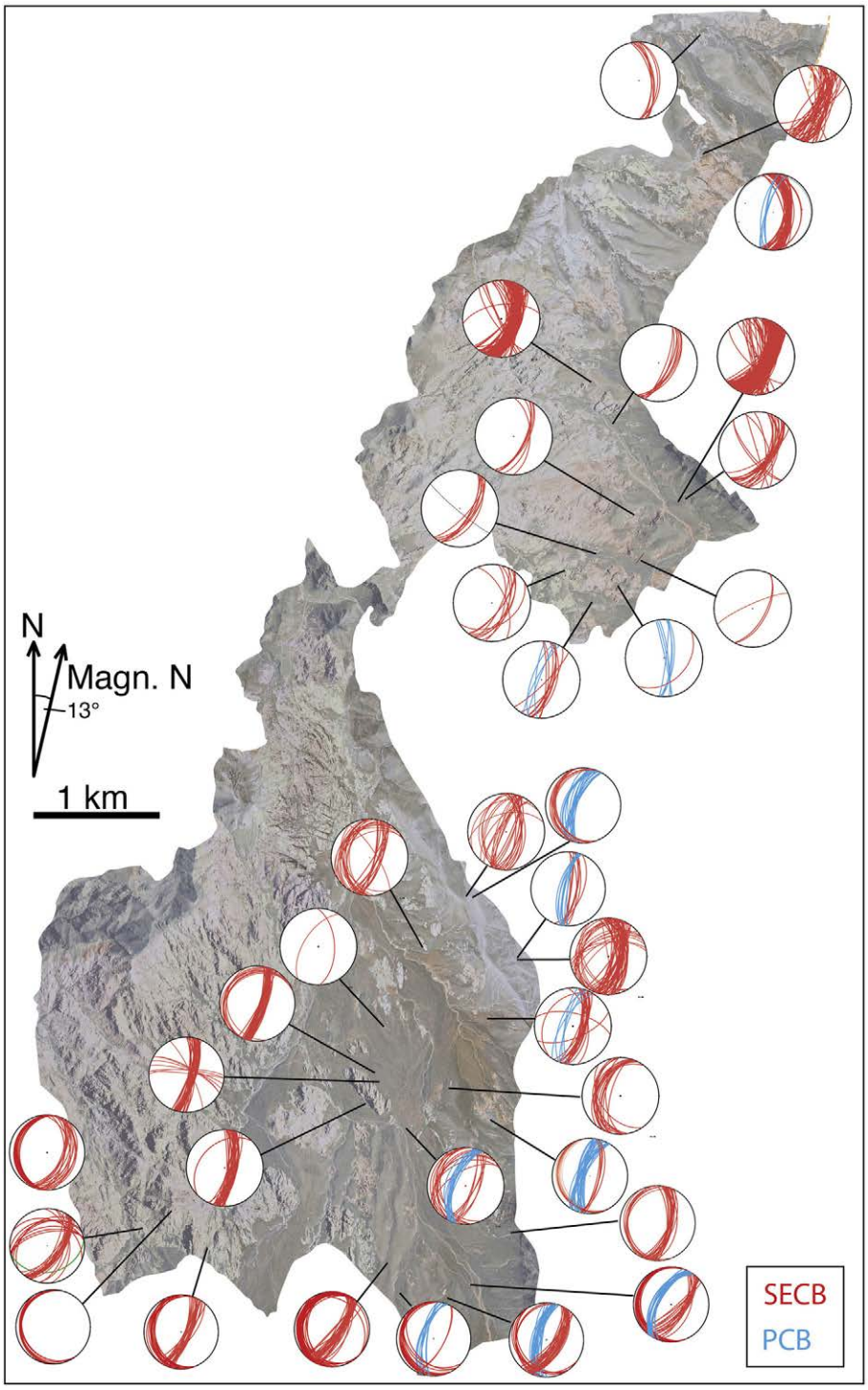

Fig. 7. Aerial photo of the Buffington Window with stereonet plots of SECB (shear-enhanced compaction bands) and PCB (pure compaction bands) orientations from selected localities.

defined network organization. These bands are sometimes specifically located at dune boundaries or dune foresets. Locally there are steep bands that offset the contractional bands, and it is possible that some steep bands may have formed during a later (Basin and Range?) phase of deformation. Locally CSBs also organize themselves into ladder structures (Davis, 1999; Schultz and Balasko, 2003) that show reverse offsets (Fig. 4f).

At the microscale, these CSBs show much stronger internal cataclasis than the PCBs and SECBs, as evidenced from significant grain-size reduction and the presence of angular small grains (Figs. 8c and 9c). Furthermore, some of the bands have developed an internal slip surface, where grain crushing is very intense (cf. Rotevatn et al., 2008). The slip surfaces are manifested by ultracataclastic zones only a fraction of a millimeter thick, showing clear striations (in general, deformation bands do not show striations). Locally they also develop into faults containing internal gouge and intense cataclasis at the boundaries of certain sand dune units. These slip surfaces exhibit striations or slickenlines from mechanically broken grains, which together with the observation of sense of slip on bands and faults can be used to constrain the shortening direction during their formation (see Section 4 below).

4. Strain and shortening direction

Deformation bands, both in general and in the study area, particularly PCBs and SECBs, are low-strain features. Also, the strain that they accommodate in the study area as a whole is very low (<0.25%), notwithstanding the fact that the sandstone has been overthrust by a large thrust sheet. Nevertheless, the deformation bands and their orientations provide information about the direction of maximum shortening. The SECBs, which formed before the CSB, show a fairly consistent pattern with a dominant E-dipping set and a subordinate W dipping one (Figs. 6 and 7). The PCBs define a single set that seems to bisect the two sets of SECBs (Fig. 6a). Hence, SECBs and PCBs together form a consistent geometric arrangement that indicates maximum shortening along a direction plunging 24° toward 101. Considering the overall E-tilted bedding caused primarily by post-Sevier Basin and Range extensional faulting, restoration of bedding to horizontal suggests an approximately horizontal shortening direction at around 100 for the Aztec sandstone both in the Buffington Window and Valley of Fire.

Some of the CSBs show central striated slip surfaces that serve as kinematic indicators. Several are parallel or make a low angle to bedding, which means that sense of slip may be difficult to determine with confidence except where they crosscut SEDBs. However, many of the striations trend E–W, suggesting E–W shortening, which is supported by kinematic analysis of the slip data (Fig. 6g) and the dihedral angle defined by conjugate sets (Figs. 1 and 6b, e). Hence, the CSBs exhibit an almost E–W shortening direction, which corresponds quite well with that extracted from the SECB and PCB orientation data.

5. Discussion and conclusions

The Jurassic Aztec sandstone in the Buffington Window, SE Nevada, is an example of porous sandstone overthrust by a nappe of older rocks in an orogenic foreland setting. The internal strain in the sandstone is very low, except for a relatively narrow zone along the Muddy Mountains thrust. It is not clear why the deformation is so strongly localized to the thrust zone. As argued by Hubbert and Rubey (1959), high fluid pressures help thrust nappes advance above their footwalls due to the related reduction in fault strength along their base. Evidence for elevated pore pressure within the thrust zone during thrusting is represented by hydraulic breccia in hanging-wall carbonates along the thrust faults. The footwall Aztec Sandstone itself must have been a very permeable footwall during thrusting, implying that fluid overpressures would not easily be developed or maintained. Nevertheless, breccia structures are also present in the sandstone in the form of vertical structures some decimeters to meters wide. Hence some overpressure must have occurred, at least locally. It is not clear if shalely layers in the carbonate-dominated rocks of the thrust nappe and/or the cataclastic and cemented thrust zone facilitated overpressure for sufficiently long periods of time that the thrust sheet could move – transport of a major thrust nappe over a thick permeable unit like the Aztec Sandstone remains enigmatic (Brock and Engelder, 1977). Regardless, mild strains are distributed also in the footwall in the form of different types of deformation bands, as further discussed below.

5.1. Distribution of bands in a contractional stress-state

The close to E–W shortening direction reflected by the orientations and kinematics of all groups of deformation bands in the Aztec sandstone is in good agreement with the Sevier shortening direction reported from this part of the Cordilleran thrust belt

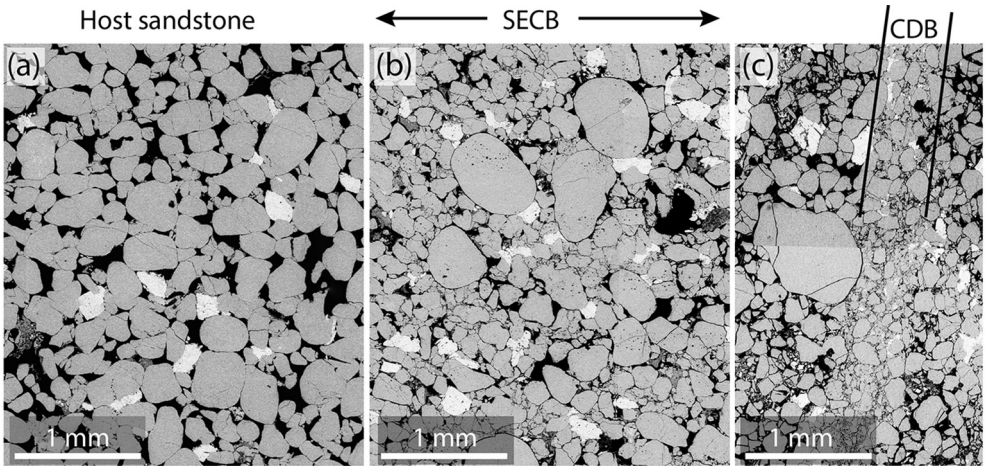

Fig. 8. SEM images of a) host sandstone, b) a nearby SECB, and c) a nearby CDB, all within 10 cm of one another. The SECB shows lower porosity and a larger fraction of small grains than the host rock. Note more intense grain-size reduction in (c). Microfractures suggests that grain size reduction is related to grain crushing, but there is also textural evidence for pressure solution.

(DeCelles, 2004). In general, the present work fit what seems to be a general pattern of contractional deformation of porous sandstones: widely distributed deformation band populations and the formation of compaction bands in highly porous sand(stones). The widely distributed occurrence of SECBs in the Buffington Window and Valley of Fire rather than localization into dense band clusters is qualitatively similar to observations made by Solum et al. (2010), Soliva et al. (2013) and Ballas et al. (2014). Their occurrence is controlled by local lithologic parameters (porosity, grain size), but where they occur, they are more or less evenly distributed with a regular spacing, a bit similar to joint distributions in competent layers (e.g., Rives et al., 1992). While the spacing of SECBs in the Buffington Window is around 3 m^{-1}, it is considerably higher in some examples of the Provence sandstones investigated by Soliva et al. (2013) and Ballas et al. (2014) (ca. 30 m^{-1}), implying a lower strain level in the Buffington Window (although the bands are thicker in the Buffington Window). To what extent the spacing of SECBs relates to bed thickness (effective bed thickness is much higher for the Aztec Sandstone), rock properties, and/or boundary conditions remains to be investigated. Chemenda et al. (2014) found that spacing also correlates with symmetry in the sense that a double set of bands (high symmetry) develops more widely spaced bands than layers with only one set of bands. For PCBs field observations show that for the Navajo Sandstone, the band density increases consistently with an increase in grain size, porosity and permeability (Fossen et al., 2011).

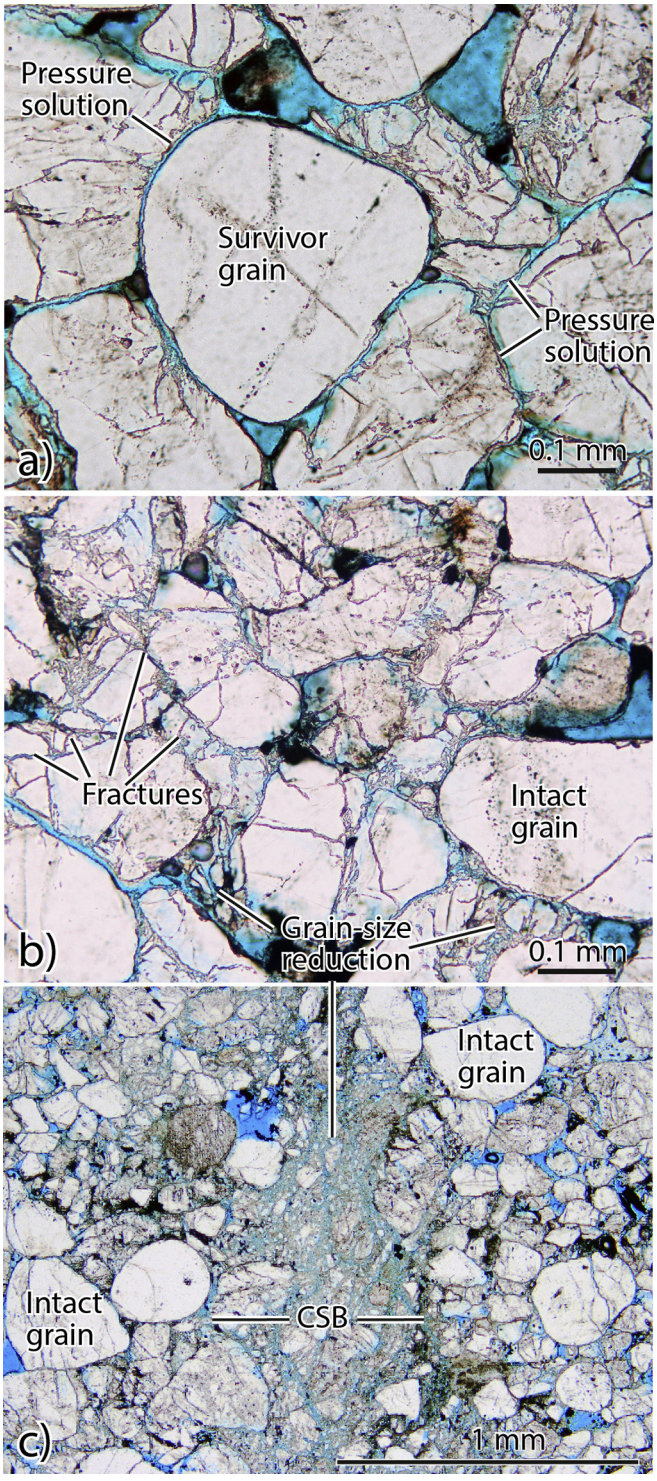

Fig. 9. Internal structure of SECB (a and b) (thin section), showing clear evidence of dissolution and grain fracture. c) Thin section view of cataclastic shear band, showing much more profound grain size reduction (evidence of grain crushing) than the SECB.

So far, shear-enhanced compaction bands (SECBs) and pure compaction bands (PCBs) have only been reported from contractional settings, notably Valley of Fire, Nevada (Sternlof et al., 2005; Eichhubl et al., 2010), Buckskin Gulch, Utah (Mollema and Antonellini, 1996; Fossen et al., 2011), and Provence, France (Ballas et al., 2013). Following Soliva et al. (2013), an explanation for this is the low differential stress associated with the contractional (or thrust) regime at shallow crustal levels. Soliva et al. (2013) discussed this in the framework of the differential stress vs. the effective mean stress, known as the q-p diagram (Fig. 11a), which is commonly used to represent state of stress and mode of deformation (e.g., Schultz and Siddharthan, 2005). This diagram is composed of a linear envelope for frictional sliding (critical state line), and an elliptical envelope or cap for compactional flow. Permanent deformation (plastic yielding) occurs when the stress path intersects the yield cap or the critical state line. The elliptical shape of the cap is defined experimentally (e.g., Zhang et al., 1990; Wong et al., 1997, 2012; Grueschow and Rudnicki, 2005), and this experimental work has shown that its intersection P* with the horizontal p-axis (Fig. 11a) depends on grain radius R and porosity ϕ through the relation $P^* = (\phi R)^{-1.5}$. In concert with Soliva et al. (2013), we follow Rudnicki (2004) and define the cap geometry as a quarter ellipse with an aspect ratio $a/b = 1.74$, where a is the maximum value of q and $b = P^*/2$. Hence, the position of the cap in the q-p diagram is defined by the local lithology (grain size and porosity), whereas the stress path is controlled by the amount of overburden (burial depth) and tectonic stress.

The mode of deformation at the onset of permanent deformation is prescribed by the point at which the stress path intersects the cap (e.g., Schultz and Siddhartan, 2005; Wibberley et al., 2007). The mode is compactional (PCBs and SECBs) in the middle part of the cap, while it is dominated by simple shear (CSBs) near the intersection between the cap and the critical state line. The expected stress path for a buried sandstone deformed in the contractional (or thrust) regime is one that reaches the yield cap in its central part (Fig. 11a). In contrast, the extensional (normal fault) regime predicts a point of intersection higher on the cap, i.e. closer to simple shear (Soliva et al., 2013) (Fig. 11a). Hence, according to this simple model, deformation bands forming in the normal regime should be shear-dominated, while they should be more compactive (SECBs and CSBs) and distributed in the contractional regime, i.e. similar to what is generally observed. The difference in localization is likely related to the amount of shear involved: numerous studies have documented clustering of shear deformation bands into zones that may or may not evolve into faults or slip surfaces, while contraction, which involves more compaction,

result in much more distributed bands. However, it is interesting to note that even the cataclastic bands in the Aztec Sandstone do not localize easily into well-defined fault structures in the area, except for specific conditions such as at dune boundaries, but appear to be distributed in the sandstone. Hence there may also be other conditions, including boundary conditions, that control the distribution of bands.

In order to utilize the q-p diagram more specifically for the Buffington Window area, we want to consider the stress conditions and rock properties at the time of deformation of the Aztec Sandstone. As a relatively well-sorted eolian sandstone unit we can assume that the porosity was high (perhaps 30%) at shallow burial depths, decreasing to the present conditions over time due to mechanical compaction and dissolution at grain contact points. However, the burial depth at the time of deformation band formation is not clear. As discussed by Brock and Engelder (1977), local clastic sediments occur between the Keystone-Muddy Mountains thrust and the Aztec Sandstone (footwall), with clasts from both Mezosoic sandstones and carbonates similar to those found in the Muddy Mountains nappe. This has led several authors to suggest that the thrust sheet moved across the earth's surface, represented by an erosional top Aztec Sandstone covered by debris from the advancing thrust sheet, i.e., a foreland basin. The thickness of this basin is unknown, but considered to be relatively thin because of the limited amounts (up to a few tens of meters) preserved in the Buffington Window (Brock and Engelder, 1977). Hence, the burial depth at the onset of contraction is uncertain, but could be very shallow, depending on the local thickness of the Sevier foreland basin. The maximum burial depth, on the other hand, is controlled by the thickness of the thrust sheet, which from stratigraphic considerations has been estimated to a minimum of 4–5 km (Brock and Engelder, 1977).

In an attempt to constrain the depth of deformation band formation, we have calculated the stress paths for the thrust regime for different cases, i.e. stress paths that initiates once the maximum horizontal stress exceeds the vertical stress and the thrust regime is entered (point (3) in Fig. 11a). This was done for the following burial depths: 0.2, 0.8, 1.4 and 2.0 km (Fig. 11b), using appropriate ratios k_0 of horizontal vs. vertical effective stress, which relates to the state of compaction of the sandstone, especially due to pressure solution and thus to the burial depth (see Soliva et al., 2013 and references therein). The extreme burial depth values chosen were 0.2 and 2 km, and these define a space of possible thrust-domain stress conditions for the sandstone (Fig. 11b, shaded area). Two caps are considered that relate to the parts of the Aztec Sandstone where SECBs are found: one for shallow burial conditions (30% porosity, grain radius of 0.25 mm) and one for maximum burial conditions (18.6%, which is the estimated current porosity, and the same grain radius of 0.25 mm). A large part of this porosity reduction is by pressure solution, which occurs at significant rates at temperatures ≥90 °C (Bjørkum et al., 1998). Hence the cap calculated for 18.6% porosity is relevant to band formation at 2–3 km burial depth and low values of k_0 (0.4), while the one calculated for 30% porosity is relevant for shallower burial and large values of k_0 (0.7). In either case, the sector of each cap that can be intersected by the stress paths is marked by a thicker green color. This sector of possible cap intersections is narrow and in the shearing-mode upper part of the cap for high burial depths (2 km), hence SECBs and PCBs are not expected to form at such burial depths. In contrast, for low burial depths and high (30%) porosity, this sector is much wider (about half the cap), suggesting that compactional bands (SECBs and PCBs) are more likely to form at these low burial conditions. Hence we conclude that the SECBs and PCBs most likely formed at relatively low burial depths, up to 1.4 km depth, which would imply that they formed before or at a relatively early stage of thrust sheet emplacement. However, the CSBs could have formed also at deeper burial depths, i.e. during overthrusting, consistent with the observed cross-cutting relationships (Fig. 4c).

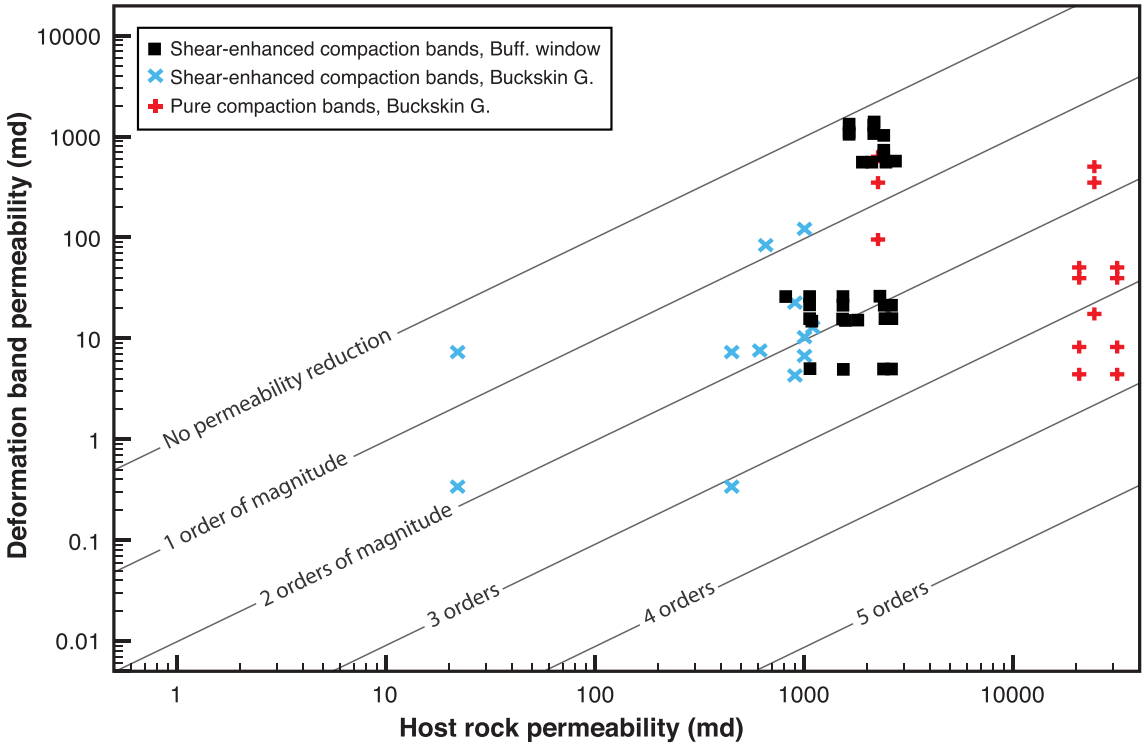

Fig. 10. Permeability measurements of shear enhanced compaction bands (SECB), Buffington Window, plotted together with measurements of SECB and compaction bands from the Buckskin Gulch area, Utah (Fossen et al., 2011). The host rock permeability is always high for PCBs because they only form in rocks with very high porosity (Fossen et al., 2011).

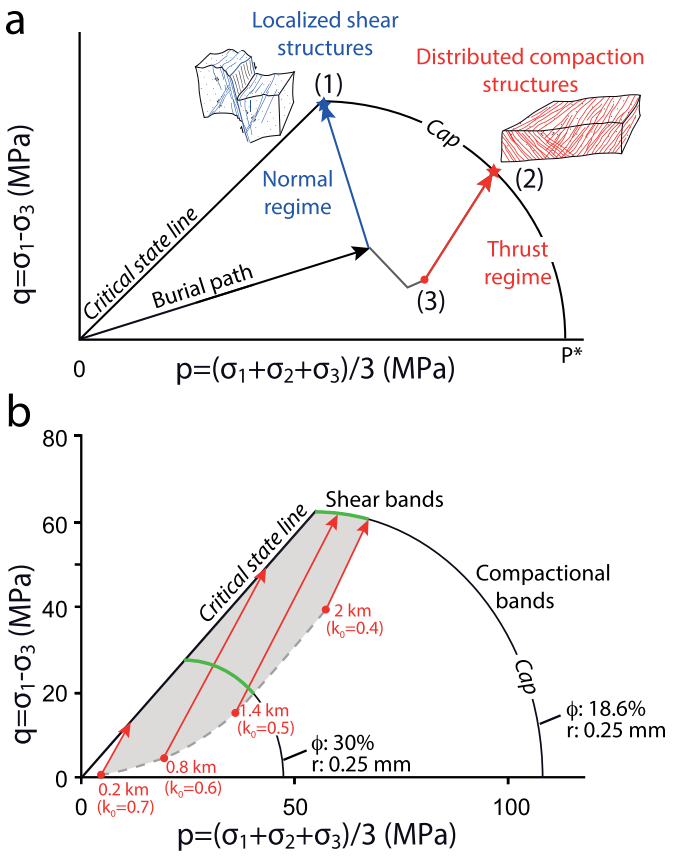

Fig. 11. a) Generalized q–p diagram with a theoretical stress path for a highly porous sand(stone) undergoing burial and then normal fault regime (blue line) or thrust regime (red line) stress evolution. Normal fault regime implies a reduction in the horizontal stress, and the path intersects the upper part of the cap (1), implying shearing. In the thrusting regime the cap is intersected in the area where compaction is important (2). b) Stress paths (corresponding to red path in a) for the thrusting regime for four cases of different burial depth and elastic properties. Two caps for porosities of 30% and 18.6% are indicated, and it is seen that SEDBs can more easily form in the high porosity case where the sector of possible cap intersections (green line) is wider. See text for discussion. (For interpretation of the references to color in this figure legend, the reader is referred to the web version of this article.)

5.2. Organization of band network

The SECBs both in the Buffington Window and Valley of Fire are organized into networks consisting of conjugate sets in isolated parts of the sandstone reservoir, typically with the E-dipping set being the dominating set. The fact that the E-dipping (foreland-dipping) conjugate set of SECBs is overall more pronounced than the W-dipping (hinterland-dipping) may seem surprising if they are related to shear stress generated by the friction on the thrust fault. However, the thrust was probably very weak, and there is no obvious strain gradient deeper than some meters into the footwall. Hence, the bands formed deeper in the footwall may more likely be related to overall Sevier-generated layer-parallel shortening before or during overthrusting. In order to explore the causal mechanisms behind this situation, we draw parallels to similar SECB populations formed in poorly consolidated sandstones in Provence, France. These sandstones deformed at shallow (<500 m) depths during mild regional contractional tectonics without the formation of major thrust nappes. SECBs in this area also form conjugate sets of bands, and also there each set is largely confined to domains rather than both sets being present in the same outcrop (Ballas et al., 2013). Ballas et al. (2013) conclude that the establishment of a set of uniformly dipping bands must have had an impeding effect on oppositely dipping bands, which would rather form in parts of the sandstone with no preexisting SECBs and that the dip direction of the bands is more or less arbitrary. A relationship between the dip direction of SECBs and the foreset of dunes is described by Deng and Aydin (2012) in Valley of Fire. These authors suggest that the dip direction is not necessarily arbitrary in the Aztec Sandstone but closely related to the anisotropy imposed by eolian cross beds. However, few of the sets in the Buffington Window directly follow eolian cross beds, hence the role of this anisotropy on set development is not immediately clear, and further exploration of this effect seems to require numerical modeling of such anisotropic sandstone.

Numerical modeling of homogeneous sandstone has been carried out by Chemenda et al. (2012, 2014). They produced populations of oppositely dipping SECBs (shear bands with an additional compactional strain perpendicular to the bands) using lithological parameters that correspond to that of the Aztec Sandstone in the Valley of Fire area. These authors used a three-layer model where a 1 m elastic–plastic layer was confined between two 0.5 m elastic layers, and where layer-parallel shortening and layer-perpendicular extension was applied. An elastic–plastic instability resulted in the formation of SECBs with symmetric or asymmetric arrangements, depending on the elastic properties of the layers and frictional properties of the layer boundaries. The numerical results demonstrate that it is possible to produce uniformly dipping SECBs (asymmetric distributions of SECBs) in the Aztec Sandstone during layer-parallel shortening (subhorizontal σ_1) (Fig. 12). In the case of the Aztec Sandstone, a difference in elasticity between dune foresets, because of their differences in grain size and porosity, could then lead to the formation of asymmetric SECB networks of the style observed in the study site. This hypothesis is supported by the formation of SECBs and PCBs in high-porosity foresets showing consequently lower elasticity whereas few or no bands are generally observed in foresets with finer grain size and lower porosity, and therefore higher elasticity. These models suggest also that a high friction at the contact between sandstone layers lead to the development of asymmetric band networks (Chemenda et al., 2014). The presence of SECBs or CSBs along the dune and foreset boundaries should increase the friction at the contact and then also lead to asymmetric network formation. The similarities to asymmetric SECB distributions in sandstones in Provence, which formed without thrusting, may suggest that these SECB populations in the Aztec Sandstone also formed prior to thrusting. However, such an arrangement of SECBs could also have formed during thrusting, provided that the orientation of σ_1 in the footwall during thrusting was close to horizontal,

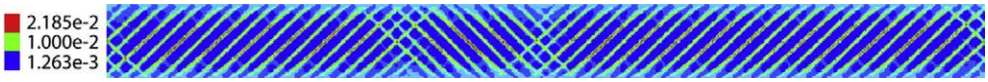

Fig. 12. Output from a plane strain finite-difference three-layer model showing the 1 m thick middle elastic–plastic layer located between two 0.5 m thick elastic layers (not shown). Layer-parallel compression generated an elastic–plastic instability that resulted in the formation of SEDBs with a preferred orientation. The figure shows variations in accumulated inelastic shear strain. Young's modulus is 10 GPa for all layers. Note large domains of uniformly-dipping bands. From Chemenda et al. (2014).

which again would depend on the friction on the thrust fault during thrusting.

5.3. Fluid flow

In terms of communication and fluid flow, the organization of SEDBs observed in the Aztec Sandstone serves to reduce permeability in the layers with the highest porosity. Their permeability reducing effect is not great enough (and the bands not close enough) to cause significant reduction of the bulk (reservoir-scale) fluid flow (Fossen and Bale, 2007), but they may still have an effect. In terms of stratigraphy, the lower parts of the dune units are the parts of highest permeability and also where SEDBs are developed. Without the SEDBs, this part of the dune unit would channelize fluid during injection-assisted production of oil and gas, and during injection of CO_2. However, the presence of SECBs at an angle to the dune boundaries in the most high-permeable part will serve to reduce the effective permeability somewhat in this zone, hence homogenize the overall permeability structure of the eolian sandstone reservoir. In this sense, the presence of SECBs in a reservoir setting makes for a more effective sweep and potentially enhance recovery. However, because they mostly strike in the same direction (N–S in the present study area), injection and production wells must be placed so that fluids flow perpendicular to the band sets, i.e. in an E–W direction in the study area, as they would have close to no effect on strike-parallel flow.

5.4. Concluding remarks

In conclusion, the Aztec Sandstone in the Buffington Window and Valley of Fire shows what may be a characteristic development for sandstones in the contractional regime: 1) Development of distributed deformation bands with very low shear displacements (SECBs and PCBs) with no tendency to cluster to create potential future fault locations. 2) Secondary formation of strongly cataclastic band that are thinner with larger shear offsets, also distributed but without network organization and often located at dune boundaries. This evolution is consistent with the expected deformation occurring in material hardened by both burial and pervasive distribution of SECBs (Schultz and Siddarthan, 2005; Wibberley et al., 2007). The main characteristics of deformation of porous sandstone in the thrusting regime, which differ from those in porous sandstone deformed in extension, are 1) the (probably early) formation of distributed deformation bands without fault localization, quite different from the more localized deformation in fault propagation folds to steeper reverse faults (Zuluaga et al., 2014) and in the extensional regime (Aydin and Johnson, 1978), and 2) the occurrence of compactional deformation bands (SECBs and PCBs), which have never been described from the extensional regime. Most of the strain and displacement, however, localized to the thrust zone, while the strain accumulated by deformation bands in the Aztec Sandstone underneath the thrust zone was very small.

Acknowledgment

This study is part of the COPS (contraction of porous sandstone) project at Center for integrated petroleum research (Uni CIPR), supported by the University of Bergen and Statoil. We are thankful for helpful review comments by Virginia Toy.

References

Antonellini, M., Aydin, A., 1994. Effect of faulting on fluid flow in porous sandstones: petrophysical properties. Am. Assoc. Petrol. Geol. Bull. 78, 355–377.
Aydin, A., Johnson, A.M., 1978. Development of faults as zones of deformation bands and as slip surfaces in sandstones. Pure Appl. Geophys. 116, 931–942.
Ballas, G., Soliva, R., Sizunb, J.-P., Fossen, H., Benedicto, A., Skurtveit, E., 2013. Shear-enhanced compaction bands formed at shallow burial conditions; implications for fluid flow (Provence, France). J. Struct. Geol. 47, 3–15.
Ballas, G., Soliva, R., Sizun, J.-P., Benedicto, A., Cavailhes, T., Raynaud, S., 2012. The importance of the degree of cataclasis in shear bands for fluid flow in porous sandstone, Provence, France. AAPG Bull. 96, 2167–2186.
Ballas, G., Soliva, R., Benedicto, A., Sizunb, J.-P., 2014. Control of tectonic setting and large-1 scale faults on the basin-scale distribution of deformation bands in porous sandstone (Provence, France). Mar. Petrol. Geol. 55, 142–159.
Bohannon, R.G., 1983. Geologic map, tectonic map, and structure sections of the Muddy and northern Black Mountains, Clark County, Nevada. In: U.S. Geological Survey Miscellaneous Investigations Series Map, I-1406, 1 sheet, scale 1:62,500.
Brock, W.G., Engelder, J.T., 1977. Deformation associated with the movement of the Muddy Mountain overthrust in the Buffington window, southeastern Nevada. Geol. Soc. Am. Bull. 88, 1667–1677.
Chemenda, A.I., Ballas, G., Soliva, R., 2014. Impact of a multilayer structure on initiation and evolution of strain localization in porous rocks: field observations and numerical modeling. Tectonophysics 631, 29–36.
Chemenda, A.I., Wibberley, C., Saillet, E., 2012. Evolution of compactive shear deformation bands: numerical models and geological data. Tectonophysics 526–529, 56–66.
Davis, G.H., 1999. Structural geology of the Colorado plateau region of southern Utah. Geol. Soc. Am. Special Pap. 342, 1–157.
DeCelles, P.G., 2004. Late jurassic to eocene evolution of the cordilleran thrust belt and foreland basin system, western U.S.A. Am. J. Sci. 304, 105–168.
Deng, S., Aydin, A., 2012. Distribution of compaction bands in 3D in an aeolian sandstone: the role of cross-bed orientation. Tectonophysics 574–575, 204–218.
Eichhubl, P., Hooker, J., Laubach, S.E., 2010. Pure and shear-enhanced compaction bands in Aztec Sandstone. J. Struct. Geol. 32, 1873–1886.
Fisher, Q.J., Knipe, R.J., 2001. The permeability of faults within siliciclastic petroleum reservoirs of the North Sea and Norwegian Continental Shelf. Mar. Petrol. Geol. 18, 1063–1081.
Fossen, H., Bale, A., 2007. Deformation bands and their influence on fluid flow. Am. Assoc. Petrol. Geol. Bull. 91, 1685–1700.
Fossen, H., Hesthammer, J., 1997. Geometric analysis and scaling relations of deformation bands in porous sandstone. J. Struct. Geol. 19, 1479–1493.
Fossen, H., Schultz, R.A., Torabi, A., 2011. Conditions and implications for compaction band formation in the Navajo Sandstone, Utah. J. Struct. Geol. 33 (10), 1477–1490.
Grueschow, E., Rudnicki, J.W., 2005. Elliptic yield cap constitutive modeling for high porosity sandstone. Int. J. Solids Struct. 42, 4574–4587.
Hesthammer, J., Fossen, H., 2001. Structural core analysis from the Gullfaks area, northern North Sea. Mar. Petrol. Geol. 18, 411–439.
Hubbert, M.K., Rubey, W.W., 1959. Role of fluid pressure in mechanics of over-thrust faulting. GSA Bull. 70, 115–166.
Johansen, S.E., Fossen, H., 2008. Internal geometry of fault damage zones in siliclastic rocks. In: Wibberley, C.A.J., Kurz, W., Imber, J., Holdsworth, R.E., Collettini, C. (Eds.), The Internal Structure of Fault Zones: Implications for Mechanical and Fluid-flow Properties, pp. 35–56, 299. Geological Society Special Publication.
Mollema, P.N., Antonellini, M.A., 1996. Compaction bands: a structural analog for anti-mode I cracks in aeolian sandstone. Tectonophysics 267, 209–228.
Rives, T., Razack, M., Petit, J.P., Rawnsley, K.D., 1992. Joint spacing: analogue and numerical simulations. J. Struct. Geol. 14, 925–937.
Rotevatn, A., Fossen, H., 2011. Simulating the effect of subseismic fault tails and process zones in a siliciclastic reservoir analogue: implications for aquifer support and trap definition. Mar. Petrol. Geol. 28, 1648–1662.
Rotevatn, A., Torabi, A., Fossen, H., Braathen, A., 2008. Slipped deformation bands: a new type of cataclastic deformation bands in Western Sinai, Suez rift, Egypt. J. Struct. Geol. 30, 1317–1331.
Rudnicki, J.W., 2004. Shear and compaction band formation on an elliptic yield cap. J. Geophys. Res. 109, 10.
Saillet, E., Wibberley, C.A.J., 2010. Evolution of cataclastic faulting in high-porosity sandstone, Bassin du Sud-Est, Provence, France. J. Struct. Geol. 32, 1590–1608.
Schultz, R.A., Balasko, C.M., 2003. Growth of deformation bands into echelon and ladder geometries. J. Geophys. Res. 30.
Schultz, R.A., Siddharthan, R., 2005. A general framework for the occurrence and faulting of deformation bands in porous granular rocks. Tectonophysics 411, 1–18.
Soliva, R., Schultz, R.A., Ballas, G., Taboada, A., Wibberley, C., Saillet, E., Benedicto, A., 2013. A model of strain localization in porous sandstone as a function of tectonic setting, burial and material properties; new insight from Provence (southern France). J. Struct. Geol. 49, 50–63.
Solum, J.G., Brandenburg, J.P., Naruk, S.J., Kostenko, O.V., Wilkins, S.J., Schultz, R.A., 2010. Characterization of deformation bands associated with normal and reverse stress states in the Navajo Sandstone, Utah. Am. Assoc. Petrol. Geol. Bull. 94, 1453–1474.
Sternlof, K., Karimi-Fard, M., Durlofsky, L.J., 2006. Flow and transport effects of compaction bands in sandstone at scales relevant to aquifer and reservoir management. Water Resour. Res. 42, 16.
Sternlof, K., Rudnicki, J.W., Pollard, D.D., 2005. Anticrack inclusion model for compaction bands in sandstone. J. Geophys. Res. 110, 16.

Tembe, S., Baud, P., Wong, T.-F., 2008. Stress conditions for the propagation of discrete compaction bands in porous sandstone. J. Geophys. Res. 113, 16.
Torabi, A., Fossen, H., Braathen, A., 2013. Insight into petrophysical properties of deformed sandstone reservoirs. AAPG Bul. 97, 619–637.
Underhill, J.R., Woodcock, N.H., 1987. Faulting mechanisms in high-porosity sandstones: new Red Sandstone, Arran, Scotland. In: Jones, M.E., Preston, R.M.F. (Eds.), Deformation of Sediments and Sedimentary Rocks, pp. 91–105, 29. Geological Society, Special Publications.
Wibberley, C.A.J., Petit, J.-P., Rives, T., 2007. The mechanics of fault distribution and localization in high-porosity sands, Provence, France. In: Lewis, H., Couples, G.D. (Eds.), The Relationship Between Damage and Localization, pp. 19–46, 289. Geological Society, London, Special Publications,.
Wong, T.-f., Baud, P., 2012. The brittle-ductile transition in porous rock: a review. J. Struct. Geol. 44, 25–53.
Wong, T.-F., David, C., Zhu, W., 1997. The transition from brittle faulting to cataclastic flow in porous sandstones: mechanical deformation. J. Geophys. Res. 102, 3009–3025.
Zhang, J., Wong, T.-F., Davis, D.D., 1990. Micromechanics of pressure-induced grain crushing in porous rocks. J. Geophys. Res. 95, 341–352.
Zuluaga, L.F., 2015. Contractional Deformation of Porous Sandstone. University of Bergen, p. 200. PhD thesis.
Zuluaga, L.F., Fossen, H., Rotevatn, A., 2014. Progressive evolution of deformation band populations during Laramide fault-propagation folding: Navajo Sandstone, San Rafael monocline, Utah, U.S.A. J. Struct. Geol. 68, 66–81.